Published in final edited form as:
Mol Cell. 2008 May 9; 30(3): 303–314. doi:10.1016/j.molcel.2008.04.002.

The Metastasis-Associated Gene *Prl-3* Is a p53 Target Involved in Cell-Cycle Regulation

Shashwati Basak[1,4], **Suzanne B.R. Jacobs**[1], **Adam J. Krieg**[1], **Navneeta Pathak**[1], **Qi Zeng**[3], **Philipp Kaldis**[3], **Amato J. Giaccia**[1], and **Laura D. Attardi**[1,2,*]

[1]Division of Radiation and Cancer Biology, Department of Radiation Oncology, Stanford University School of Medicine, Stanford, CA 94305, USA

[2]Department of Genetics, Stanford University School of Medicine, Stanford, CA 94305, USA

[3]Institute of Molecular and Cell Biology, Proteos, Singapore 138673

SUMMARY

The p53 tumor suppressor restricts tumorigenesis through the transcriptional activation of target genes involved in cell-cycle arrest and apoptosis. Here, we identify *Prl-3* (*p*hosphatase of *r*egenerating *l*iver-*3*) as a p53-inducible gene. Whereas previous studies implicated Prl-3 in metastasis because of its overexpression in metastatic human colorectal cancer and its ability to promote invasiveness and motility, we demonstrate here that Prl-3 is an important cell-cycle regulator. Consistent with a role in DNA damage-induced cell-cycle arrest, Prl-3 overexpression induces G_1 arrest downstream of p53 by triggering a PI3K-Akt-activated negative feedback loop. Surprisingly, attenuation of Prl-3 expression also elicits an arrest response, suggesting that basal level Prl-3 expression is pivotal for normal cell-cycle progression. Our findings highlight key dose-dependent functions of Prl-3 in both positive and negative regulation of cell-cycle progression and provide insight into Prl-3's role in cancer progression.

INTRODUCTION

The p53 tumor suppressor plays a critical role in protecting organisms from developing cancer (Vousden and Lu, 2002). The ability of p53 to inhibit tumorigenesis is attributed to p53's activity as a cellular stress sensor, as diverse stress signals, including DNA damage, hypoxia, and oncogene expression, lead to p53 activation (Ryan et al., 2001). Activation of p53 can provoke different cellular responses, including G_1 cell-cycle arrest, senescence, or apoptosis, any of which can impede tumor development by preventing the expansion of neoplastic cells.

p53 is a transcription factor that activates and represses a multitude of target genes proposed to participate in the cell-cycle arrest or apoptotic responses (Vousden and Lu, 2002). Genetic data obtained from mice lacking specific p53 target genes, such as *p21* or *Bax*, indicate their importance as mediators of p53-dependent cell-cycle arrest and apoptosis, respectively (Brugarolas et al., 1995; Deng et al., 1995; Knudson et al., 1995). Further, the requirement for transactivation by p53 for triggering at least some of its cellular responses is emphasized

*Correspondence: attardi@stanford.edu.
[4]Present address: Department of Urology, VA Medical Center, San Francisco, CA 94121, USA.

SUPPLEMENTAL DATA

Supplemental Data include four figures and can be found with this article online at http://www.molecule.org/cgi/content/full/30/3/303/DC1/.

by the inability of a transactivation-deficient p53 mutant to activate apoptosis in response to DNA damage (Chao et al., 2000; Johnson et al., 2005). Thus, the identification of p53 target genes is key for elucidating how p53 engages specific cellular programs, including cell-cycle arrest, senescence, and apoptosis.

Although a number of transcriptional targets of p53 have been identified, our knowledge of p53 effector functions remains incomplete (Vousden and Lu, 2002). For example, although p21 clearly participates in the G_1 checkpoint response, $p21^{-/-}$ mouse embryonic fibroblasts (MEFs) are only partially deficient in the G_1 arrest elicited by p53, suggesting the existence of additional p53-dependent targets involved in cell-cycle regulation (Brugarolas et al., 1995; Deng et al., 1995). Similarly, other than *Pml and Pai-1*, the genes required for p53-induced senescence remain unknown (de Stanchina et al., 2004; Kortlever et al., 2006). Furthermore, given that cells deficient for p53 apoptotic target genes typically display only partially compromised apoptosis, it is probable that there remain to be identified other mediators critical for p53-dependent apoptosis (Ihrie and Attardi, 2004). Hence, there are likely to be additional undiscovered p53-inducible genes involved in mediating these different p53 responses.

To identify additional downstream effectors of p53, we performed a microarray analysis on primary mouse fibroblasts exposed to DNA damage. To enhance the likelihood of discovering new p53 target genes, we chose to examine the endogenous p53 response to DNA damage in primary cells, in contrast to most previous screens used to identify p53-inducible genes, which have relied on p53 overexpression in human cancer cell lines with a variety of genetic lesions. Using this approach, we describe here the identification of *Prl-3* (*p*hosphatase of *r*egenerating *l*iver-*3*) as a direct p53 target gene (Zeng et al., 1998). Previously, Prl-3 was shown to be overexpressed during the transition to metastasis in human colorectal cancer development, and ectopic expression of Prl-3 in cells promoted cell invasiveness and motility as well as metastasis in mouse models (Saha et al., 2001; Zeng et al., 2003). Thus, *Prl-3* was of particular interest given the apparent paradox of being activated by p53 yet being involved in metastasis. Here, through analysis of Prl-3 activity in primary cells, we reveal an additional facet of Prl-3 function. Our studies demonstrate a pivotal role for Prl-3 in cell-cycle regulation, thereby providing fundamental insight into Prl-3's role in tumor development.

RESULTS

Prl-3 Is Induced in a p53-Dependent Manner

To identify p53 target genes, we performed microarray analysis on wild-type and *p53*-deficient MEFs after treatment with the DNA damaging agent Doxorubicin (Dox; Jacobs et al., 2007). After initial analysis of expression profiles, we focused on the *Prl-3* gene, both because of its apparent p53 dependence and its reported role in carcinogenesis (Saha et al., 2001). In particular, studies have suggested a critical role for Prl-3 in promoting cancer metastasis through effects on cell migration and invasion (Zeng et al., 2003). We first verified that Prl-3 is induced by DNA damage in a p53-dependent manner at both the RNA and protein levels (Figures 1A and 1B). Notably, we observed *Prl-3* induction both in MEFs and in E1A oncogene-expressing MEFs, which undergo cell-cycle arrest and apoptosis, respectively, after Dox treatment, consistent with a potential role in either pathway (Figure 1A). To assess how broadly *Prl-3* is induced by p53, we examined its activation in response to other DNA damaging agents and in different cell types. We found that *Prl-3* is induced in wild-type, but not $p53^{-/-}$, MEFs treated with UVC, demonstrating that distinct DNA damaging agents activate *Prl-3* expression in a p53-dependent manner (Figure 1C). Additionally, *Prl-3* was upregulated by p53 in other cell types, as γ irradiation led to *Prl-3* induction in wild-type, but not $p53^{-/-}$, thymocytes (Figure 1D). Furthermore, LTR6 mouse

myeloid leukemia cells expressing a temperature-sensitive p53 mutant (Jacobs et al., 2007) showed enhanced *Prl-3* expression simply after p53 activation by temperature shift to 32°C, in the absence of genotoxic stress (Figure 1E). Together, these experiments demonstrate that *Prl-3* is induced upon p53 activation in different contexts, supporting the notion that it is a bona fide p53 target.

Prl-3 Is a Direct Target of p53

To establish whether *Prl-3* is a direct transcriptional target of p53, we scanned the mouse *Prl-3* genomic region spanning 6.0 kb upstream of the transcriptional start site through the third exon for potential p53-binding sites. We identified two putative p53-binding sites in the first and second introns (BS1 and BS2, respectively, Figure 2A). We also identified a putative p53-binding site in the human *PRL-3* genomic region, in an analogous position to BS1 in mouse *Prl-3* with respect to the start of the first coding exon, suggesting that this site is conserved between mouse and human and supporting the idea that BS1 is a functional p53 regulatory site for *Prl-3* in vivo (Figure S1A available online). We performed electrophoretic mobility shift assays to determine whether p53 can bind to BS1 or BS2 of the mouse *Prl-3* gene. With extracts from Dox-treated wild-type, but not $p53^{-/-}$, MEFs we observed a shift with BS1, indicating that p53 binds this element (Figure 2B). Binding of p53 to BS1 was competed by wild-type BS1 oligonucleotides, but not by BS1 oligonucleotides carrying mutations in critical p53 consensus site residues, demonstrating the specificity of the interaction. In contrast, we did not observe p53 binding to the BS2 site (Figure S1B). We confirmed the binding of p53 to BS1 in vivo by chromatin immunoprecipitation, which revealed a 5-fold enhancement in p53 binding to BS1 upon Dox treatment of wild-type MEFs, mirroring the increase in *Prl-3* message levels (Figures 2C and 1A).

To assess whether p53 can directly activate transcription of *Prl-3*, we generated a *Prl-3* reporter construct, Prl-3-BS1, comprising 1.3 kb upstream of the transcriptional start site, exon 1, and a portion of intron 1 encompassing BS1 upstream of the firefly luciferase gene (Figure 2D). We also generated another construct, Prl-3-MutBS1, in which BS1 was mutated at key p53 consensus nucleotides. To determine the responsiveness of the wild-type *Prl-3* regulatory region to endogenous p53, we introduced Prl-3-BS1 into both wild-type and $p53^{-/-}$ MEFs. We observed a 35-fold induction of luciferase activity with the Prl-3-BS1 construct in wild-type MEFs compared to $p53^{-/-}$ MEFs, confirming that the *Prl-3* regulatory region responds to p53 (Figure 2E). Mutation of BS1 completely abrogates this response, demonstrating that the observed p53-dependent activity is mediated through this site. To test the responsiveness of the *Prl-3* reporter to human p53, we utilized p53-deficient H1299 human lung adenocarcinoma cells reconstituted with exogenous human p53. Activity of Prl-3-BS1 was enhanced 2.5-fold in the presence of p53 relative to the vector control, whereas Prl-3 Mut-BS1 failed to respond to p53 (Figure 2F). Together, these results demonstrate that *Prl-3* is a direct transcriptional target of p53 in both mouse and human cells.

Prl-3 Expression Triggers G_1 Cell-Cycle Arrest in Primary Cells

Activation of p53 elicits two main cellular responses: cell-cycle arrest—either temporary or permanent—and apoptosis (Vousden and Lu, 2002). To decipher Prl-3's function downstream of p53, we examined the consequences of Prl-3 expression on cell proliferation and viability in MEFs. We expressed HA-tagged Prl-3 in wild-type MEFs and observed that Prl-3 displays plasma membrane-associated localization, consistent with earlier studies (Figures 3A and 4B; Zeng et al., 2003). Cell-cycle progression in Prl-3-expressing MEFs was examined by quantifying BrdU incorporation in comparison to non-Prl-3-expressing cells (Figures 3A and 3B). p53- and β-galactosidase-expressing MEFs served as positive and

negative controls, respectively, as expression of p53 is known to provoke an arrest in these cells, whereas β-galactosidase expression fails to do so (Attardi et al., 1996). As expected, p53 triggered a robust arrest in MEFs, whereas β-galactosidase had no effect on cell proliferation (Figure 3B). Interestingly, we found that Prl-3 expression decreases the BrdU labeling index to an extent similar to p53, reflecting cell-cycle arrest activity (Figures 3A and 3B). Moreover, Prl-3 expression triggers a cell-cycle arrest response in *p53*$^{-/-}$ MEFs, suggesting that Prl-3 acts downstream of p53 in inducing arrest.

To delineate the phase of the cell cycle in which Prl-3 expression induces arrest, we examined centrosome status by immunostaining for γ-tubulin. The presence of a single γ-tubulin focus representing one centrosome is indicative of the G_1 phase of the cell cycle, whereas two foci reflect the S or G_2/M phases (Stearns, 2001). The numbers of γ-tubulin-positive foci were quantified both in Prl-3-expressing and nonexpressing MEFs. In contrast to the nonexpressing MEFs, which commonly displayed two γ-tubulin foci, greater than 70% of the Prl-3-expressing MEFs stained positive for one γ-tubulin focus, indicating that cells arrested by Prl-3 are in G_1 (Figures 3C and 3D). Together, these data demonstrate that Prl-3 expression in MEFs is sufficient to elicit a G_1 arrest downstream of p53. In contrast, expression of HA-Prl-3 in wild-type MEFs had no effect on cell viability, indicating that Prl-3 is not sufficient to induce apoptosis (data not shown).

Our findings demonstrating growth-suppressive properties of Prl-3 in primary fibroblasts contrast with previous studies in tumor cells suggesting that Prl-3 is an oncogene. For example, Prl-3 expression in transformed human embryonic kidney cells enhances proliferation (Matter et al., 2001). We reasoned that Prl-3 might have different activities in primary cells maintaining intact genetic pathways compared to cancer cells that have undergone numerous alterations en route to malignancy. To address this hypothesis, we examined the effect of Prl-3 overexpression on cell proliferation of human tumor cell lines. We found that, in contrast to p53, Prl-3 was unable to induce arrest in some cancer cell lines, including human RKO colon carcinoma cells and U2OS osteosarcoma cells (Figure 3E and Figure S2A). In other human cancer cell lines, such as human HT1080 fibrosarcoma cells, Prl-3's arrest capacity remained intact (Figure 3E and Figure S2B). These findings support the idea that Prl-3-mediated arrest is highly dependent on genetic context and suggests that its ability to trigger cell-cycle arrest can be lost during tumorigenesis.

Prl-3-Induced Cell-Cycle Arrest Is Associated with Inhibition of the PI3K-Akt Pathway

Recently, it was shown that Prl-3 expression in human colorectal cancer cells can lead to activation of the PI3K-Akt pathway, known for enhancing both cell proliferation and cell migration (Wang et al., 2007). Consistent with this notion, we detected Prl-3 at the plasma membrane, both at the endogenous level and when overexpressed in MEFs and HT1080 cells (Figures 4A and 4B). To elucidate how Prl-3 expression induces G_1 arrest, we examined the status of this pathway by analyzing Akt phosphorylation, a marker of PI3K activation, at different time points after Prl-3 expression. As reported previously, we found that low levels of Prl-3 resulted in PI3K-Akt pathway activation, reflected by an increase in phospho-Akt (Figure 4C, lane 2). Surprisingly, however, as Prl-3 protein accumulated to high levels with time, we observed a decrease in activated Akt (Figure 4C, lane 3), reminiscent of the recently described finding that PI3K activation leads to engagement of a negative feedback loop that ultimately inhibits PI3K-Akt signaling and leads to growth arrest (Courtois-Cox et al., 2006). To examine whether Prl-3-induced arrest relies on a functional Akt pathway, we expressed Prl-3 in *Akt1*$^{-/-}$*;Akt2*$^{-/-}$ MEFs and assessed the status of the cell cycle by BrdU incorporation. Indeed, we observed that Prl-3 was unable to arrest these MEFs (Figures 4D and 4E), indicating that Akt is essential for Prl-3-induced cell-cycle arrest. To determine whether subsequent attenuation of the PI3K-Akt pathway

could contribute to the observed Prl-3-induced cell-cycle arrest, we assessed whether Prl-3 affects the critical downstream cell-cycle effectors of Akt specifically involved in G_1-S progression. In response to activated Akt, Foxo transcription factors are phosphorylated and excluded from the nucleus, allowing cell-cycle progression. As a result of Akt inhibition, Foxo proteins translocate to the nucleus and induce growth arrest by transcriptionally activating cell-cycle regulatory genes, including the *p21* and *p27* cyclin-dependent kinase inhibitors (CDKIs; Burgering and Kops, 2002). In keeping with an inhibition of Akt driven by Prl-3, we found that Prl-3 expression in HT1080 cells resulted in a dramatic increase in the percentage of cells with nuclear Foxo3a as well as an upregulation of p21 and p27 (Figure 4F–4H), reflective of active Foxo capable of inhibiting cell-cycle progression. In addition, Akt is known to phosphorylate and inactivate p21 function by cytosolic retention (Zhou et al., 2001). Expression of Prl-3 in HT1080 cells led to an increase in the percentage of cells with nuclear p21, consistent with Prl-3 causing a G_1 arrest via inhibition of Akt (Figures 4I and 4J). Together, these results suggest that Prl-3-induced arrest relies on Akt activation followed by negative feedback regulation of the PI3K-Akt pathway.

Prl-3 Enforces Cell-Cycle Arrest Downstream of the Restriction Point via Cdk2

Our finding that Prl-3 expression is associated with induction of the p21 and p27 CDKIs suggested that Prl-3 may activate cell-cycle arrest through effects on CDKs. Progression from G_1 to S relies on both Cdk4 and Cdk2: Cdk4/cyclin D is required to inactivate the Rb family of proteins at the restriction point, whereas Cdk2/cyclin E is required not only to inactivate Rb family members but also to activate other proteins such as p220 (NPAT) and nucleophosmin, which are critical for histone synthesis and centrosome duplication, respectively (Lundberg and Weinberg, 1998; Ma et al., 2000; Okuda et al., 2000). To determine how Prl-3 impinges upon the cell-cycle machinery, we first examined whether Prl-3 exerts its effects at the restriction point. Triple knockout (TKO) MEFs deficient for all three Rb family members (Rb, p107, and p130) fail to undergo G_1 arrest in response to a number of signals, including DNA damage, contact inhibition, and growth factor deprivation (Sage et al., 2000). To determine if Prl-3 can induce arrest in the absence of the Rb family members, we expressed Prl-3 in TKO MEFs and assessed cell-cycle arrest (Figure 5A). Intriguingly, Prl-3 expression can enforce an arrest in TKO MEFs commensurate with that seen upon p53 overexpression, suggesting that Prl-3 acts downstream of the restriction point to elicit an arrest response. In keeping with this notion, Prl-3 arrested MEFs lacking Cdk4 (Figure 5B). In contrast, we found that Prl-3 was greatly compromised in inducing arrest in *Cdk2*$^{-/-}$ MEFs (Figure 5B; Berthet et al., 2003). Consistent with an effect at the level of Cdk2, Prl-3-induced arrest was impaired in MEFs lacking p21 (Figure 5B). Moreover, ectopic co-expression of Cdk2/cyclin E with Prl-3 was able to fully rescue the arrest elicited by Prl-3 alone (Figure 5C and Figure S3). These findings together suggest that Prl-3 triggers cell-cycle arrest in late G_1, downstream of Rb and the restriction point, via effects on Cdk2.

Prl-3 Knockdown Induces Cell-Cycle Arrest in a p53-Dependent Manner

Having determined that ectopic expression of Prl-3 is sufficient for G_1 arrest, we next sought to examine the consequences of Prl-3 deficiency for cell-cycle progression. Toward this end, we designed several retroviral constructs expressing different shRNAs directed against mouse *Prl-3* (designated A–D). Upon identifying two *Prl-3* shRNAs, A and C, that could effectively attenuate expression of overexpressed HA-Prl-3 (Figure 6A), we examined the ability of these hairpins to knock down endogenous Prl-3 by retrovirally transducing wild-type MEFs with empty vector viruses or viruses expressing shRNA A, shRNA C, or a nonspecific (NS) shRNA control and then treating with Dox to induce high-level Prl-3 expression. Both Prl-3 mRNA and protein levels were diminished in MEFs infected with retroviruses expressing either the A or C shRNAs, but not control viruses, demonstrating the efficacy of endogenous Prl-3 knockdown using these shRNAs (Figures 6B and 6C).

To ascertain whether Prl-3 knockdown affects cell-cycle progression in unstressed cells, wild-type and $p53^{-/-}$ MEFs were infected with empty vector viruses or viruses expressing the *Prl-3* A, *Prl-3* C, or NS shRNAs and then analyzed by two-dimensional BrdU/PI cell-cycle FACS analysis (Brugarolas et al., 1995). Surprisingly, suppression of Prl-3 in wild-type MEFs with either the A or C shRNAs resulted in a decreased S phase fraction compared to cells transduced with empty vector or NS shRNA controls (Figures 6D and 6E). In striking contrast, knockdown of Prl-3 had no effect on the S phase fraction of $p53^{-/-}$ MEFs (Figure 6F). These results demonstrate that attenuating Prl-3 expression causes cell-cycle arrest that relies on an intact p53 pathway.

Prl-3 Knockdown Leads to Upregulation of p53 via the $p19^{Arf}$ Pathway in Unstressed Cells

Because the arrest ensuing from Prl-3 ablation in MEFs depends on p53, we hypothesized that Prl-3 knockdown may result in augmented p53 activity. To address this idea, we first examined p53 protein levels in untreated wild-type MEFs upon Prl-3 knockdown. Compared to both the vector and NS shRNA controls, MEFs with diminished Prl-3 displayed higher p53 protein levels (Figure 7A). To define the basis for p53 accumulation in Prl-3 knockdown MEFs, we examined the two main pathways that lead to p53 stabilization. DNA damage can induce p53 stabilization through the activation of kinases that phosphorylate p53 on serines 18 and 23, thereby displacing the Mdm2 ubiquitin ligase, a negative regulator of p53 (Vousden and Lu, 2002). Alternatively, induction of $p19^{Arf}$, an upstream positive regulator of p53, leads to p53 stabilization by sequestering Mdm2 (Sherr, 2006). To assess the first possibility, we examined serine 18 phosphorylation of p53. We found no change in the levels of serine18-phosphorylated p53 upon Prl-3 ablation in unstressed wild-type MEFs, suggesting that stimulation of the DNA damage pathway does not account for the enhanced p53 levels (Figure 7A). In contrast, we found that MEFs with diminished Prl-3 displayed enhanced $p19^{Arf}$ protein levels compared to control cells, suggesting that $p19^{Arf}$-mediated sequestration of Mdm2 might result in increased p53 protein stability (Figure 7B). To assess the requirement for $p19^{Arf}$ in the p53-dependent arrest observed in the absence of Prl-3, we examined the cell-cycle profile of $p19^{Arf-/-}$ MEFs after Prl-3 knockdown. This analysis showed no change in the S phase fraction after Prl-3 ablation, indicating that the arrest phenotype observed with decreased Prl-3 depends on an intact $p19^{Arf}$-Mdm2-p53 pathway (Figure 7C). We found further that arrest upon Prl-3 knockdown was associated with activation of p38 MAPK, a cytoplasmic kinase shown previously to activate $p19^{Arf}$, suggesting a potential mode through which Prl-3 loss could induce $p19^{Arf}$ upregulation (Figure 7D; Bulavin et al., 2004; Ito et al., 2006). Furthermore, p53 stabilization in this context resulted in enhanced p53 transcriptional activity, as evidenced by *p21* and *Mdm2* induction upon Prl-3 knockdown (Figure 7E). Together, these results suggest that downregulation of Prl-3 in unstressed MEFs leads to induced p53 transcriptional activity via increased p53 protein levels.

To gain mechanistic insight into downstream components of the arrest response triggered by Prl-3 knockdown, we assessed whether p21, a central mediator of p53-dependent cell-cycle arrest, is required for the observed arrest. $p21^{-/-}$ MEFs with diminished Prl-3 expression displayed a partial compromise in cell-cycle arrest relative to wild-type MEFs (compare Figures 7F and 6E), suggesting that *p21* and at least one additional p53 target gene are involved in eliciting a complete p53-dependent arrest response upon Prl-3 knockdown. Together, our data suggest that basal Prl-3 expression is important to ensure cell-cycle progression and that, in its absence, cells undergo a $p19^{Arf}$-p53-p21-dependent arrest.

DISCUSSION

Here, we describe the identification of a previously reported metastasis-associated gene, *Prl-3*, as a p53-regulated gene with a pivotal role in cell-cycle regulation. Our observation that overexpression of Prl-3 induces G_1 arrest is consistent with the idea that Prl-3 participates in DNA damage-induced, p53-dependent cell-cycle arrest. We demonstrate further that Prl-3 ablation also triggers arrest, suggesting a role for basal Prl-3 levels in promoting cell cycling. Thus, our studies highlight critical dose-sensitive effects of Prl-3 expression on cell-cycle progression.

To gain insight into p53-mediated cell-cycle arrest, we sought to delineate the signaling pathway through which Prl-3 overexpression blocks cell-cycle progression. As it was previously reported that Prl-3 can activate PI3K signaling (Wang et al., 2007), we examined whether engagement of the PI3K pathway contributed to Prl-3-induced arrest. Indeed, we found that low-level Prl-3 expression resulted in activation of the PI3K substrate Akt, and furthermore, by employing Akt-deficient MEFs, we found that Akt is a requisite component of Prl-3-induced cell cycle arrest. However as PI3K-Akt signaling is associated typically with proliferation, this observation presented a paradox. A resolution came from the discovery that with the accumulation of higher levels of Prl-3 occurring during arrest, PI3K-Akt signaling was inhibited. Such transient activation of Akt by low levels of Prl-3, followed by attenuation of Akt signaling with high levels of Prl-3, is reminiscent of the negative feedback inhibition of PI3K-Akt responsible for triggering senescence of human fibroblasts in response to activated oncogene expression (Courtois-Cox et al., 2006). In support of such a mechanism for Prl-3-induced arrest, we found that the arrest elicited by Prl-3 displays features characteristic of cell-cycle arrest resulting from Akt inhibition, including nuclear localization of the Foxo3a transcription factor, upregulation of the p21 and p27 CDKIs, and p21 nuclear localization. We showed further that Prl-3's point of action is downstream of the restriction point, as Prl-3 arrests MEFs lacking Rb family members as well as MEFs deficient for Cdk4, which is essential for inactivating Rb. In contrast, we found that Prl-3-induced arrest activity is partially compromised in both *Cdk2*$^{-/-}$ and *p21*$^{-/-}$ MEFs, suggesting that this arrest response depends on Cdk2. Beyond phosphorylating Rb, Cdk2 phosphorylates other substrates, including proteins essential for histone synthesis and centrosome duplication (Ma et al., 2000; Okuda et al., 2000), and is clearly required for G_1-S progression downstream of the restriction point. Hence, as a direct target of p53, Prl-3 likely blocks cell proliferation by triggering a PI3K-Akt-activated negative feedback loop, ultimately impinging upon Cdk2 to induce an arrest downstream of Rb (Figure S4A).

Interestingly, we discovered that knockdown of endogenous Prl-3 in unstressed cells provokes a p53-dependent cell-cycle arrest. This arrest is associated with enhanced p53 protein levels and transcriptional activity, an effect mediated via p19^{Arf}, an important upstream activator of p53 engaged by diverse stimuli, including hyperproliferative signals and oxidative stress (Sherr, 2006). These results suggest that, normally, basal Prl-3 expression in unstressed MEFs facilitates cell-cycle progression (Figure S4B). Two different models can be envisioned to explain the signaling pathway(s) linking Prl-3 loss to p53 activation. In one model, Prl-3 performs a dedicated role in a specific cellular function important for proper cell-cycle progression, and Prl-3 ablation leads to arrest via upregulation of the p19^{Arf}-p53 pathway as part of a safeguard mechanism designed to prevent aberrant cellular proliferation. Consistent with this finding, upon Prl-3 depletion, we observed upregulation of the p38 stress-induced kinase, which is known to cause p19^{Arf} induction (Bulavin et al., 2004; Ito et al., 2006). Alternatively, Prl-3 may keep p53 in check directly through negative regulation of p53 protein accumulation. The regulation of p53 via

autoregulatory feedback loops is well precedented: Mdm2, Pirh2, COP1, and Wip1 are allp53 targets involved in downregulating p53 protein levels (Harris and Levine, 2005).

It is intriguing that *Prl-3* is both a p53 target gene and a metastasis-associated gene. Apart from being upregulated in metastatic cancer relative to nonmetastatic colorectal cancer in humans, PRL-3 has biological activities related to metastasis, including the ability to promote cell invasion and migration as well as metastasis in mouse models (Saha et al., 2001; Zeng et al., 2003). Our data demonstrate an additional function for Prl-3 in cell-cycle regulation in primary cells, both when expressed at basal levels and as a p53-inducible target. Whereas basal Prl-3 levels may facilitate normal cell cycling, high levels of Prl-3 provoke an arrest, emphasizing the importance of proper modulation of Prl-3 protein levels to ensure normal cell-cycle progression. Such dose-sensitive functions for key cell-cycle regulators are not unprecedented. Notably, at normal cellular levels, PI3K promotes proliferation, but altering its expression levels can have profound effects on cells. For example, hyperactivation of the PI3K pathway, such as through ablation of the PI3K-negative regulator Pten, can induce senescence as a safeguard against inappropriate oncogene expression (Chen et al., 2005; Kim et al., 2007). Similarly, as discussed above, attenuation of PI3K signaling can also lead to senescence (Courtois-Cox et al., 2006). Hence, any inappropriate level of PI3K signaling is associated with a growth-arrest response. Akin to the senescence responses engaged by oncogene activation, the arrest induced by Prl-3 overexpression may have evolved in normal cells as a failsafe mechanism against excessive Prl-3, which could potentially promote inappropriate cycling. In contrast, in the backdrop of myriad mutations present in cancer cells, high-level Prl-3 expression may fail to trigger a cell-cycle arrest, thereby allowing other activities of Prl-3 to prevail. This hypothesis is supported by our data demonstrating that Prl-3 overexpression fails to arrest RKO and U2OS tumor cells.

The exact mode of Prl-3 action as an oncogene during tumor metastasis is currently unclear. Several recent studies have demonstrated Prl-3's ability to regulate multiple signaling cascades, including the PI3K-Akt, Rho, and Csk/Src pathways, crucial for both cell-cycle progression and cell migration (Fiordalisi et al., 2006; Liang et al., 2007; Wang et al., 2007). Depending on the constellation of signaling pathways altered in a particular cancer, Prl-3 overexpression could promote carcinogenesis either by enhancing cell motility and invasiveness or, alternatively, facilitating cell-cycle progression. Such duality of action in these processes is reminiscent of that of other proteins, such as FAK, which regulates both cell migration and cell proliferation (Cox et al., 2006). Future studies of Prl-3 will lead to a better understanding of its role in the p53 pathway as well as in metastasis.

EXPERIMENTAL PROCEDURES

Cell Culture

MEFs were generated from E13.5 embryos as described (Johnson et al., 2005). γ irradiation was performed with a ^{137}Cesium source. UV irradiation was performed as described (Johnson et al., 2005). Dox (Sigma) was added to the culture medium at a final concentration of 0.2 μg/ml. All cells were grown in DMEM with 10% FCS.

Cloning and Sequence Analysis of *Prl-3* Genomic DNA

A 321 bp fragment from *Prl-3* exon 2 was used to probe a murine genomic Bac library (Bac Pac Resources Center). Isolated clones were sequenced, and intron-exon boundaries were determined by comparison to the cDNA sequence. The *Prl-3* genomic DNA sequence was scanned for the presence of consensus p53-binding sites (el-Deiry et al., 1992). A 2.7 kb XbaI-SmaI genomic fragment containing exon 1 and the *Prl-3* p53-binding site 1 (BS1) was

cloned into the pGL3 luciferase-reporter plasmid (Promega) to generate Prl-3-BS1. The Prl-3-MutBS1 construct was generated by mutating the CXXG bases of the *Prl-3* p53-binding site to TXXC by site-directed mutagenesis (Promega).

Northern Blot Analysis

Total RNA from cells was prepared with Trizol (Invitrogen). Northern blotting was performed according to standard protocols. *Gapdh* served as a loading control.

Electrophoretic Mobility Shift Assays

EMSAs were performed as described (Johnson et al., 2005). Oligonucleotides used were *Prl-3* BS1, 5′-GGGTAGACTCAGGCATGCTGTGGGCATGCCCCTTTTTGCCC-3′; *Prl-3* BS2, 5′-ACCACATGGCAAACATGATCTGATCAGGGTTCAGGGTGTG-3′; and *p21*-5′, 5′-TGGCCATCAGGAACATGTCCCAACATGTTGAGCTCTGGCA-3′; and their respective complementary strands. Mutant competitor oligonucleotides had base substitutions in the most conserved p53 consensus binding site nucleotides (CXXG to TXXC) in both half sites.

Chromatin Immunoprecipitation Assays

Chromatin immunoprecipitation was performed as described (Hammond et al., 2006). CM5 antibodies (Vector Laboratories) were used for immunoprecipitation of p53 from cells. Primer sequences were as follows: *Prl-3* BS1, 5′GTGCGGTCCAGGAGGTAAGAC3′ and 5′CAGGCCTGAGGGGATGGAGCC3′, and control, 5′CCTAGGTGCTGCAAGGGTGAG3′ and 5′GTTCAGAACCCAGAACGGCCT3′.

Luciferase Assays

Luciferase assays were performed with the Dual Luciferase System (Promega). Twenty-five thousand MEFs or H1299 cells were plated per well in 24-well plates 12 hr prior to transfection. Seven-hundred fifty nanogram pGL3-based reporter and 62.5 ng pRLnull Renilla luciferase plasmid were transfected into each well of MEFs. For H1299 cells, 125 ng reporter, 62.5 ng pRLnull, and 125 ng of either empty pCMV or pCMV-p53 plasmid were transfected into cells. Cells were lysed 24 hr posttransfection, and assays were carried out according to the manufacturer's protocol. Firefly luciferase readings were divided by Renilla luciferase readings to control for variations in transfection efficiency.

Western Blot Analysis

Protein extracts from MEFs and HT1080 cells were prepared in RIPA buffer, and western blotting was carried out with standard protocols. Rabbit polyclonal anti-HA antibodies (Zymed) and a Prl-3-specific monoclonal antibody (clone 318; Li et al., 2005) were used for detection of HA-tagged and endogenous Prl-3 proteins, respectively. Antibodies directed against p53 (CM5; Vector Laboratories), phosphoserine 18 of p53 (Cell Signaling), $p19^{Arf}$ (Novus Biologicals), p21 (C-19, Santa Cruz Biotechnology Inc), p27 (BD Transduction), Akt, p-Akt, p38 MAPK, and p-p38 MAPK (Cell Signaling) were also used. α-tubulin or GAPDH served as loading controls.

Immunofluorescence and BrdU Assays

The pCS2-HA-Prl-3 and pCS2-GFP-Prl-3 expression vectors were constructed by PCR amplifying the Prl-3 ORF from a Prl-3 I.M.A.G.E. clone and cloning into the EcoR1/XhoI sites of the pCS2 vector containing an N-terminal HA or GFP epitope. The KA-Prl-3-HA expression vector was constructed similarly by cloning the Prl-3 ORF into the KA vector containing a C-terminal HA epitope (Jacobs et al., 2007). MEFs were plated on coverslips

and transfected with FuGENE (Roche). Twenty-four hours posttransfection, MEFs were immunostained for Prl-3 (HA, 1:250, Zymed, or when specified, clone 318 Prl-3 antibody, 1:400; Li et al., 2005), p53 (FL-393, 1:250, Santa Cruz Biotechnology), β-galactosidase (1:250, 5′-3′ Inc.), cyclin D1 (M2, 1:100, Cell Signaling), p21 (C-19, 1:10, Santa Cruz Biotechnology Inc), or γ-tubulin (GTU-88, 1:500, Sigma). For the BrdU immunofluorescence assays, MEFs were transfected with expression plasmids and 24 hr later were incubated with 3 μg/ml BrdU for 4 hr. MEFs were then fixed for double immunostaining with antigen-specific antibodies and BrdU antibodies (1:50, BD Biosciences) as described (Attardi et al., 1996). At least 100 cells were counted for each condition in each experiment unless otherwise specified.

Retroviral Infections, RNA Interference, and Cell-Cycle Analysis

The sequences of the shRNAs used in this study are as follows: A, 5′-TGCCACCCTCAGCACGTTC-3′; B, 5′-GTACGGGGCTCACACTGTG-3′; C, 5′-CAGCAAGCAGCTCACCTAC-3′; D, 5′-GACCAGATGCTGCGTCATG-3′; and NS, 5′-ACTGTTTCTCCAGGCGACT-3′. Oligonucleotides with these sequences were cloned into the pSIRIPP (*s*elf-*i*nactivating, *R*NA interference, *p*gk-*p*uro) retroviral vector (Gozani et al., 2003). Retroviral infection was performed as described (Johnson et al., 2005). After infection, MEFs were selected with 2 μg/ml of puromycin for 5 days and then replated at 10^6 cells per 10 cm plate for the BrdU/PI cell-cycle analysis. Twelve hours later, cells were treated with 3 μg/ml BrdU for 4 hr and then processed for cell-cycle analysis as described (Brugarolas et al., 1995).

Supplementary Material

Refer to Web version on PubMed Central for supplementary material.

Acknowledgments

We thank S. Artandi for the *p19*$^{Arf-/-}$ MEFs, N. Hay for the *Akt1-/;Akt2*$^{-/-}$ MEFs, S. Lessnick for the pSIRIPP plasmid, P. Jackson for the pCS2 plasmid, A. Brunet for the FLAG-Foxo3a plasmid, and T. Stearns for the γ-tubulin antibody. We thank S. Artandi, J. Sage, A. Brunet, R. Shaw, and T. M. Johnson for critically reading the manuscript. We thank T.M. Johnson and B.T. Nguyen for technical help. This work was supported by a Stanford Dean's postdoctoral fellowship and a Susan G. Komen postdoctoral fellowship to S.B., the Giannini Family Foundation to S.B.R.J., and the Damon Runyon Cancer Research Foundation and the Donald E. and Delia B. Baxter Foundation to L.D.A.

References

Attardi LD, Lowe SW, Brugarolas J, Jacks T. Transcriptional activation by p53, but not induction of the p21 gene, is essential for oncogene-mediated apoptosis. EMBO J. 1996; 15:3693–3701. [PubMed: 8758936]

Berthet C, Aleem E, Coppola V, Tessarollo L, Kaldis P. Cdk2 knockout mice are viable. Curr Biol. 2003; 13:1775–1785. [PubMed: 14561402]

Brugarolas J, Chandrasekaran C, Gordon JI, Beach D, Jacks T, Hannon GJ. Radiation-induced cell cycle arrest compromised by p21 deficiency. Nature. 1995; 377:552–557. [PubMed: 7566157]

Bulavin DV, Phillips C, Nannenga B, Timofeev O, Donehower LA, Anderson CW, Appella E, Fornace AJ Jr. Inactivation of the Wip1 phosphatase inhibits mammary tumorigenesis through p38 MAPK-mediated activation of the p16(Ink4a)-p19(Arf) pathway. Nat Genet. 2004; 36:343–350. [PubMed: 14991053]

Burgering BM, Kops GJ. Cell cycle and death control: long live Forkheads. Trends Biochem Sci. 2002; 27:352–360. [PubMed: 12114024]

Chao C, Saito S, Kang J, Anderson CW, Appella E, Xu Y. p53 transcriptional activity is essential for p53-dependent apoptosis following DNA damage. EMBO J. 2000; 19:4967–4975. [PubMed: 10990460]

Chen Z, Trotman LC, Shaffer D, Lin HK, Dotan ZA, Niki M, Koutcher JA, Scher HI, Ludwig T, Gerald W, et al. Crucial role of p53-dependent cellular senescence in suppression of Pten-deficient tumorigenesis. Nature. 2005; 436:725–730. [PubMed: 16079851]

Courtois-Cox S, Genther Williams SM, Reczek EE, Johnson BW, McGillicuddy LT, Johannessen CM, Hollstein PE, MacCollin M, Cichowski K. A negative feedback signaling network underlies oncogene-induced senescence. Cancer Cell. 2006; 10:459–472. [PubMed: 17157787]

Cox BD, Natarajan M, Stettner MR, Gladson CL. New concepts regarding focal adhesion kinase promotion of cell migration and proliferation. J Cell Biochem. 2006; 99:35–52. [PubMed: 16823799]

de Stanchina E, Querido E, Narita M, Davuluri RV, Pandolfi PP, Ferbeyre G, Lowe SW. PML is a direct p53 target that modulates p53 effector functions. Mol Cell. 2004; 13:523–535. [PubMed: 14992722]

Deng C, Zhang P, Harper JW, Elledge SJ, Leder P. Mice lacking p21CIP1/WAF1 undergo normal development, but are defective in G1 checkpoint control. Cell. 1995; 82:675–684. [PubMed: 7664346]

el-Deiry WS, Kern SE, Pietenpol JA, Kinzler KW, Vogelstein B. Definition of a consensus binding site for p53. Nat Genet. 1992; 1:45–49. [PubMed: 1301998]

Fiordalisi JJ, Keller PJ, Cox AD. PRL tyrosine phosphatases regulate rho family GTPases to promote invasion and motility. Cancer Res. 2006; 66:3153–3161. [PubMed: 16540666]

Gozani O, Karuman P, Jones DR, Ivanov D, Cha J, Lugovskoy AA, Baird CL, Zhu H, Field SJ, Lessnick SL, et al. The PHD finger of the chromatin-associated protein ING2 functions as a nuclear phosphoinositide receptor. Cell. 2003; 114:99–111. [PubMed: 12859901]

Hammond EM, Mandell DJ, Salim A, Krieg AJ, Johnson TM, Shirazi HA, Attardi LD, Giaccia AJ. Genome-wide analysis of p53 under hypoxic conditions. Mol Cell Biol. 2006; 26:3492–3504. [PubMed: 16611991]

Harris SL, Levine AJ. The p53 pathway: positive and negative feedback loops. Oncogene. 2005; 24:2899–2908. [PubMed: 15838523]

Ihrie RA, Attardi LD. Perp-etrating p53-dependent apoptosis. Cell Cycle. 2004; 3:267–269. [PubMed: 14726658]

Ito K, Hirao A, Arai F, Takubo K, Matsuoka S, Miyamoto K, Ohmura M, Naka K, Hosokawa K, Ikeda Y, Suda T. Reactive oxygen species act through p38 MAPK to limit the lifespan of hematopoietic stem cells. Nat Med. 2006; 12:446–451. [PubMed: 16565722]

Jacobs SB, Basak S, Murray JI, Pathak N, Attardi LD. Siva is an apoptosis-selective p53 target gene important for neuronal cell death. Cell Death Differ. 2007; 14:1374–1385. [PubMed: 17464332]

Johnson TM, Hammond EM, Giaccia A, Attardi LD. The p53QS transactivation-deficient mutant shows stress-specific apoptotic activity and induces embryonic lethality. Nat Genet. 2005; 37:145–152. [PubMed: 15654339]

Kim JS, Lee C, Bonifant CL, Ressom H, Waldman T. Activation of p53-dependent growth suppression in human cells by mutations in PTEN or PIK3CA. Mol Cell Biol. 2007; 27:662–677. [PubMed: 17060456]

Knudson CM, Tung KS, Tourtellotte WG, Brown GA, Korsmeyer SJ. Bax-deficient mice with lymphoid hyperplasia and male germ cell death. Science. 1995; 270:96–99. [PubMed: 7569956]

Kortlever RM, Higgins PJ, Bernards R. Plasminogen activator inhibitor-1 is a critical downstream target of p53 in the induction of replicative senescence. Nat Cell Biol. 2006; 8:877–884. [PubMed: 16862142]

Li J, Guo K, Koh VW, Tang JP, Gan BQ, Shi H, Li HX, Zeng Q. Generation of PRL-3- and PRL-1-specific monoclonal antibodies as potential diagnostic markers for cancer metastases. Clin Cancer Res. 2005; 11:2195–2204. [PubMed: 15788667]

Liang F, Liang J, Wang WQ, Sun JP, Udho E, Zhang ZY. PRL3 promotes cell invasion and proliferation by down-regulation of Csk leading to Src activation. J Biol Chem. 2007; 282:5413–5419. [PubMed: 17192274]

Lundberg AS, Weinberg RA. Functional inactivation of the retinoblastoma protein requires sequential modification by at least two distinct cyclin-cdk complexes. Mol Cell Biol. 1998; 18:753–761. [PubMed: 9447971]

Ma T, Van Tine BA, Wei Y, Garrett MD, Nelson D, Adams PD, Wang J, Qin J, Chow LT, Harper JW. Cell cycle-regulated phosphorylation of p220(NPAT) by cyclin E/Cdk2 in Cajal bodies promotes histone gene transcription. Genes Dev. 2000; 14:2298–2313. [PubMed: 10995387]

Matter WF, Estridge T, Zhang C, Belagaje R, Stancato L, Dixon J, Johnson B, Bloem L, Pickard T, Donaghue M, et al. Role of PRL-3, a human muscle-specific tyrosine phosphatase, in angiotensin-II signaling. Biochem Biophys Res Commun. 2001; 283:1061–1068. [PubMed: 11355880]

Okuda M, Horn HF, Tarapore P, Tokuyama Y, Smulian AG, Chan PK, Knudsen ES, Hofmann IA, Snyder JD, Bove KE, Fukasawa K. Nucleophosmin/B23 is a target of CDK2/cyclin E in centrosome duplication. Cell. 2000; 103:127–140. [PubMed: 11051553]

Ryan KM, Phillips AC, Vousden KH. Regulation and function of the p53 tumor suppressor protein. Curr Opin Cell Biol. 2001; 13:332–337. [PubMed: 11343904]

Sage J, Mulligan GJ, Attardi LD, Miller A, Chen S, Williams B, Theodorou E, Jacks T. Targeted disruption of the three Rb-related genes leads to loss of G(1) control and immortalization. Genes Dev. 2000; 14:3037–3050. [PubMed: 11114892]

Saha S, Bardelli A, Buckhaults P, Velculescu VE, Rago C, St Croix B, Romans KE, Choti MA, Lengauer C, Kinzler KW, Vogelstein B. A phosphatase associated with metastasis of colorectal cancer. Science. 2001; 294:1343–1346. [PubMed: 11598267]

Sherr CJ. Divorcing ARF and p53: an unsettled case. Nat Rev Cancer. 2006; 6:663–673. [PubMed: 16915296]

Stearns T. Centrosome duplication. a centriolar pas de deux. Cell. 2001; 105:417–420. [PubMed: 11371338]

Vousden KH, Lu X. Live or let die: the cell's response to p53. Nat Rev Cancer. 2002; 2:594–604. [PubMed: 12154352]

Wang H, Quah SY, Dong JM, Manser E, Tang JP, Zeng Q. PRL-3 down-regulates PTEN expression and signals through PI3K to promote epithelial-mesenchymal transition. Cancer Res. 2007; 67:2922–2926. [PubMed: 17409395]

Zeng Q, Hong W, Tan YH. Mouse PRL-2 and PRL-3, two potentially prenylated protein tyrosine phosphatases homologous to PRL-1. Biochem Biophys Res Commun. 1998; 244:421–427. [PubMed: 9514946]

Zeng Q, Dong JM, Guo K, Li J, Tan HX, Koh V, Pallen CJ, Manser E, Hong W. PRL-3 and PRL-1 promote cell migration, invasion, and metastasis. Cancer Res. 2003; 63:2716–2722. [PubMed: 12782572]

Zhou BP, Liao Y, Xia W, Spohn B, Lee MH, Hung MC. Cytoplasmic localization of p21Cip1/WAF1 by Akt-induced phosphorylation in HER-2/neu-overexpressing cells. Nat Cell Biol. 2001; 3:245–252. [PubMed: 11231573]

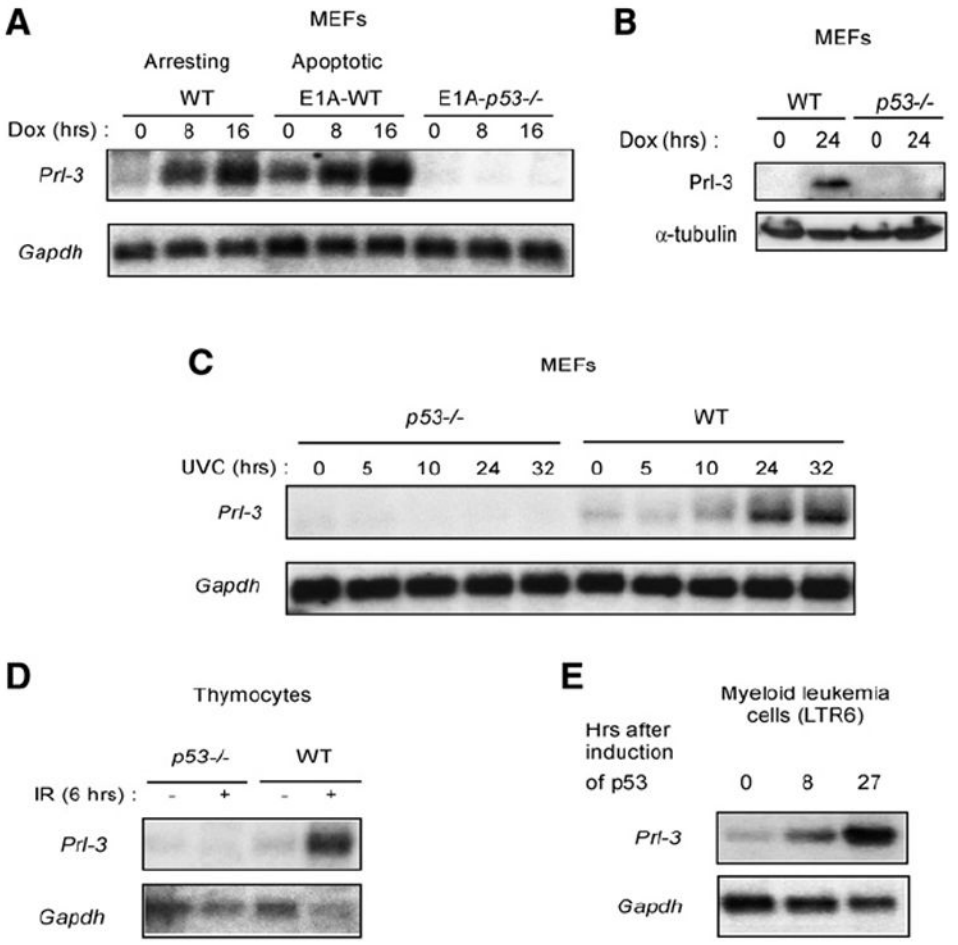

Figure 1. *Prl-3* Is Induced by p53 in a Variety of Contexts

(A) Northern blot demonstrating *Prl-3* mRNA induction in MEFs undergoing p53-mediated G_1 arrest and E1A-MEFs undergoing apoptosis in response to Doxorubicin (Dox) treatment, but not in Dox-treated E1A-$p53^{-/-}$ MEFs.

(B) Western blot showing Prl-3 protein induction in wild-type MEFs treated with Dox, but not in Dox-treated $p53^{-/-}$ MEFs.

(C) Northern blot showing that UVC light (20 J/m^2) leads to *Prl-3* induction in wild-type, but not $p53^{-/-}$, MEFs.

(D) Northern blot showing that γ irradiation (5 Gy) results in *Prl-3* activation in wild-type, but not $p53^{-/-}$, mouse thymocytes 6 hr after treatment.

(E) Northern blot showing *Prl-3* induction in LTR6 mouse myeloid leukemia cells after temperature shift from 37°C to 32°C to activate p53.

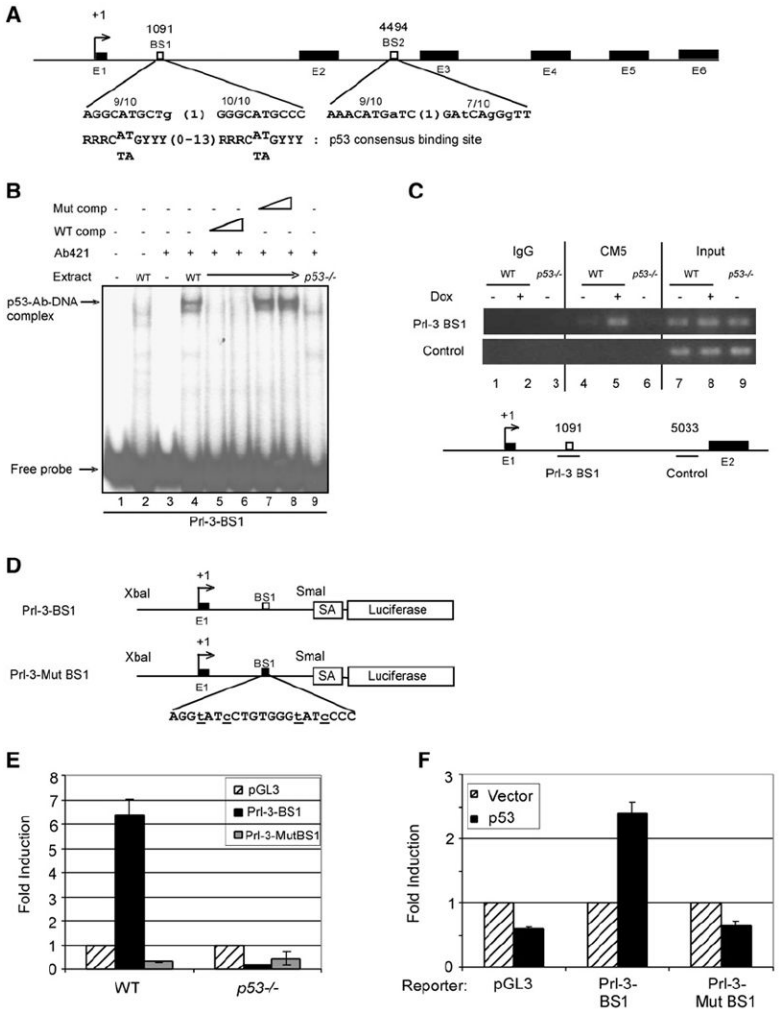

Figure 2. *Prl-3* Is a Direct p53 Target Gene

(A) Structure of the mouse *Prl-3* locus showing the exon-intron organization. Two potential p53-binding sites, BS1 and BS2, are indicated within the first and second introns of the *Prl-3* gene. The position of each site with respect to the transcription start site (+1) is indicated. BS1 and BS2 are compared to the consensus p53 binding site sequence below, with lowercase letters indicating deviations from the consensus and the numbers above the sequence indicating the number of bases matching the half sites of the consensus p53-binding site.

(B) p53 binds to the BS1 element from the *Prl-3* regulatory region. Electrophoretic mobility shift assays were performed with double-stranded (ds) oligonucleotides containing the putative p53-binding site BS1 and extracts from Dox-treated wild-type or $p53^{-/-}$ MEFs, in the presence or absence of 30- and 60-fold molar excess of either unlabeled wild-type (WT comp) or mutant (Mut comp) competitor oligonucleotides.

(C) p53 binds to the *Prl-3* BS1 element in vivo. Ethidium bromide-stained agarose gels show PCR products of the *Prl-3* BS1 site region after chromatin immunoprecipitation with a p53 antibody (CM5) or mouse IgG as a negative control on wild-type (WT) and $p53^{-/-}$ MEFs. MEFs were either left untreated or treated with Dox for 8 hr. Control indicates a region ~4.0 kb downstream of BS1 amplified by PCR as a negative control. Input represents 0.01% of the total chromatin used in the assay. A schematic of the *Prl-3* genomic region with the BS1 site and control region is shown below.

(D) Schematic of *Prl-3* luciferase reporter constructs. The Prl-3-BS1 and Prl-3-MutBS1 constructs comprising 1.3 kb upstream of the start site, exon 1, and either the wild-type or mutant p53-binding site within intron 1 upstream of luciferase are shown. The mutant p53-binding site with point mutations indicated in lowercase letters and underlined is shown below. SA denotes a splice acceptor sequence.

(E) *Prl-3* BS1 confers p53 responsiveness to the *Prl-3* luciferase reporter in MEFs. Luciferase assays were performed in wild-type ($p53^{+/+}$) and $p53^{-/-}$ MEFs after transfection with pGL3, Prl-3-BS1, or Prl-3-MutBS1. The luciferase activity of each reporter construct is shown relative to the pGL3 vector in either wild-type or $p53^{-/-}$ MEFs. The data represent the average of three independent experiments performed in duplicate, and error bars indicate the standard error of the mean (SEM).

(F) The *Prl-3* BS1 luciferase reporter construct is responsive to human p53. H1299 cells were cotransfected either with a pCMV human p53 expression plasmid (p53) or a pCMV empty vector (Vector) along with pGL3, Prl-3-BS1, or Prl-3-MutBS1 reporters. Values shown with each luciferase reporter construct in the presence of p53 are relative to the empty vector control and are the average of three independent experiments performed in duplicate, ± SEM.

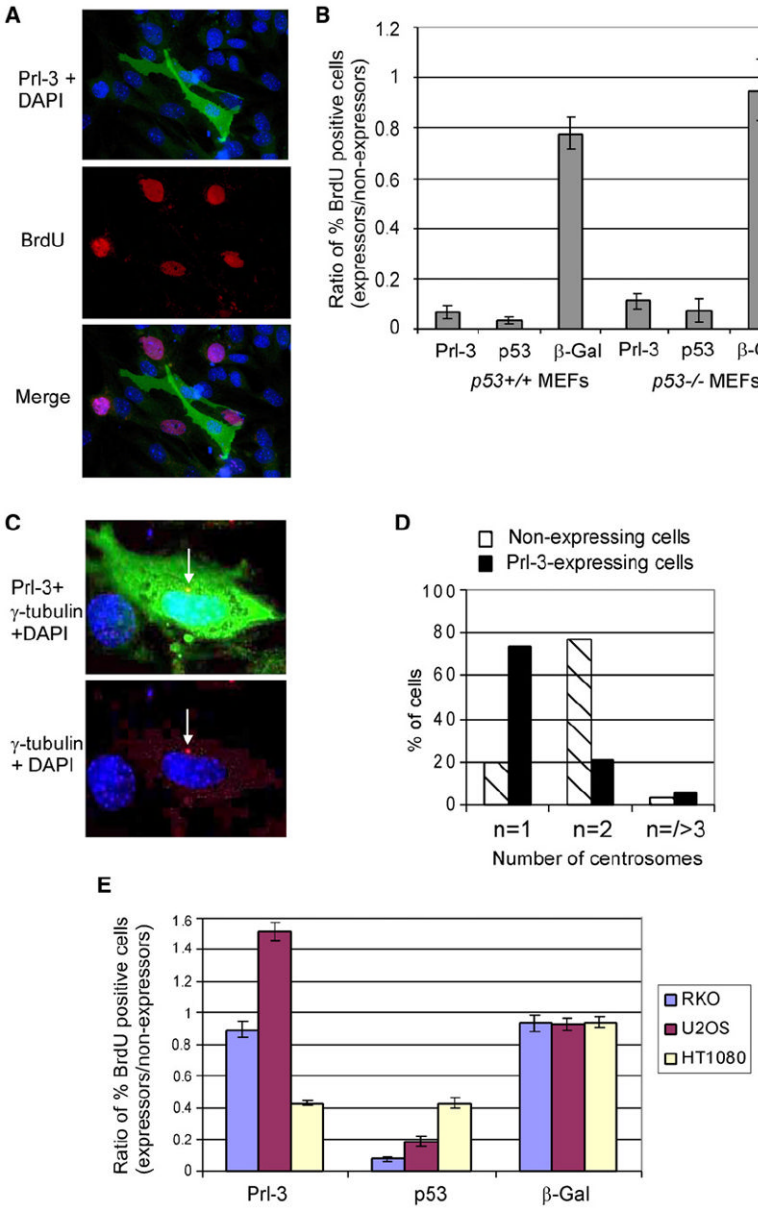

Figure 3. Prl-3 Induces G_1 Cell-Cycle Arrest in MEFs

(A and B) Prl-3 expression induces cell-cycle arrest. BrdU incorporation in MEFs expressing Prl-3-HA, p53, or β-galactosidase (β-gal) was quantified. Prl-3-induced arrest is shown by immunofluorescence in (A) and in the graph in (B), which displays the average ratios of the percentage of BrdU-positive nuclei in $p53^{+/+}$ and $p53^{-/-}$ MEFs expressing Prl-3-HA, p53, or β-gal to the percentage of BrdU-positive nonexpressing cells in each case. The data represent the average of three different experiments, ± SEM.

(C and D) MEFs expressing Prl-3 display one γ-tubulin focus indicative of G_1 arrest. (C) Immunofluorescence for γ-tubulin in Prl-3-HA-expressing wild-type MEFs, and (D) graph showing the percentages of MEFs with different centrosome numbers, as established by counting the number of γ-tubulin foci in Prl-3-HA-expressing wild-type MEFs and nonexpressing MEFs. A total of 100 cells from two experiments were counted for each condition.

(E) Prl-3 fails to arrest RKO and U2OS cells but can arrest HT1080 cells. The graph is as described in (B), with data representing the average of three independent experiments, ± SEM.

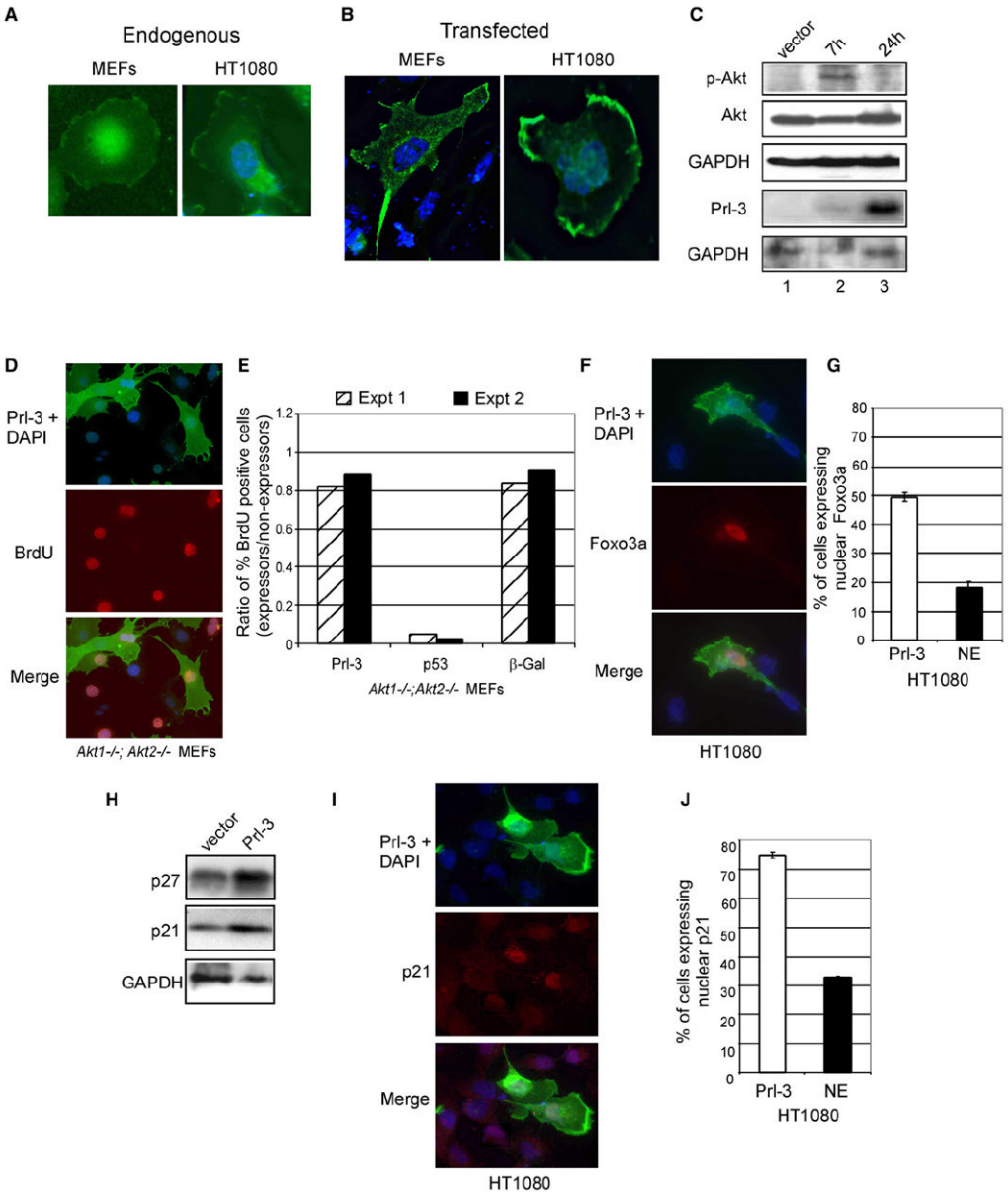

Figure 4. Prl-3-Induced Cell-Cycle Arrest Is Mediated via Inhibition of the Akt Pathway

(A) Endogenous Prl-3 localizes to the cell membrane in both wild-type MEFs synchronized in G_0 by serum starvation followed by plating on fibronectin and collagen and asynchronous human HT1080 fibrosarcoma cells.

(B) Transfected HA-Prl-3, detected with Prl-3 antibodies, is highly enriched at the plasma membrane of MEFs and HT1080 cells.

(C) Overexpression of Prl-3 leads to Akt activation, then inhibition. Western blot analysis shows the levels of Akt and phospho-Akt (p-Akt) in HT1080 cells transfected with HA-Prl-3 and analyzed at the indicated time points.

(D and E) Prl-3 fails to arrest *Akt1*$^{-/-}$;*Akt2*$^{-/-}$ MEFs. BrdU incorporation in MEFs expressing HA-Prl-3, p53, or β-gal was quantified. (D) Example of immunofluorescence, and (E) graph displaying the ratios of the percentage of BrdU-positive nuclei in *Akt1*$^{-/-}$;*Akt2*$^{-/-}$ MEFs expressing HA-Prl-3, p53, or β-gal to the percentage of BrdU-

positive nonexpressing cells in each case. The data shown represent two independent experiments.

(F and G) Expression of Prl-3 induces nuclear localization of Foxo3a. HT1080 cells cotransfected with HA-Prl-3 and FLAG-Foxo3a were immunostained for Prl-3 and Foxo3a with HA and FLAG antibodies, respectively. (F) Example of immunofluorescence, and (G) graph showing the average percentages of HA-Prl-3-expressing (Prl-3) and nonexpressing (NE) cells displaying nuclear Foxo3a from three independent experiments, ± SEM.

(H) Western blot analysis shows increased p21 and p27 protein levels in Prl-3-expressing HT1080 cells compared to vector control.

(I and J) Expression of Prl-3 induces p21 nuclear localization. HA-Prl-3-expressing HT1080 cells were immunostained for Prl-3 and p21 with Prl-3 and p21 antibodies, respectively. (I) Example of immunofluorescence and (J) graph showing the percentages of p21-positive nuclei in HA-Prl-3-expressing (Prl-3) and nonexpressing (NE) cells. The data represent the average of three independent experiments, ± SEM.

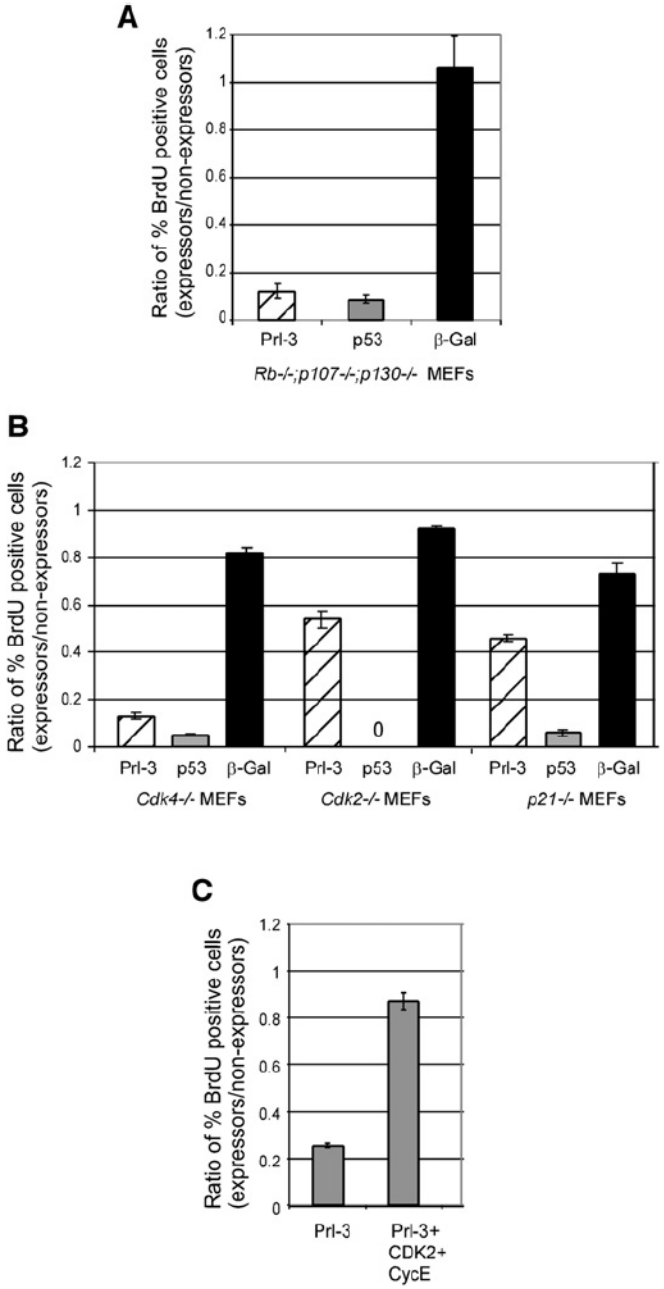

Figure 5. Prl-3-Mediated Arrest Occurs beyond the Restriction Point and Is Dependent on Cdk2

(A) Prl-3 induces an arrest in triple knockout (TKO) MEFs lacking Rb, p107, and p130. The graph shows the average ratios of the percentage of BrdU-positive TKO MEFs expressing HA-Prl-3, p53, or β-gal to the percentage of BrdU-positive, nonexpressing MEFs in each case. The data represent the average of three different experiments, ± SEM.

(B) Prl-3-mediated cell-cycle arrest is greatly compromised in *Cdk2*$^{-/-}$ and *p21*$^{-/-}$ MEFs. The graph is as described in (A). *Cdk2*$^{-/-}$ MEFs expressing p53 displayed no BrdU positivity as denoted by "0" in the graph. The data represent the average of three independent experiments, ± SEM.

(C) Cdk2/cyclin E overexpression rescues the Prl-3-induced arrest. The graph shows the average ratios of the percentage of BrdU-positive nuclei in either GFP-Prl-3 or GFP-

Prl-3+Cdk2/cyclin E coexpressing MEFs to the percentage of BrdU-positive, nonexpressing MEFs in each case. The data represent the average of three independent experiments, ± SEM.

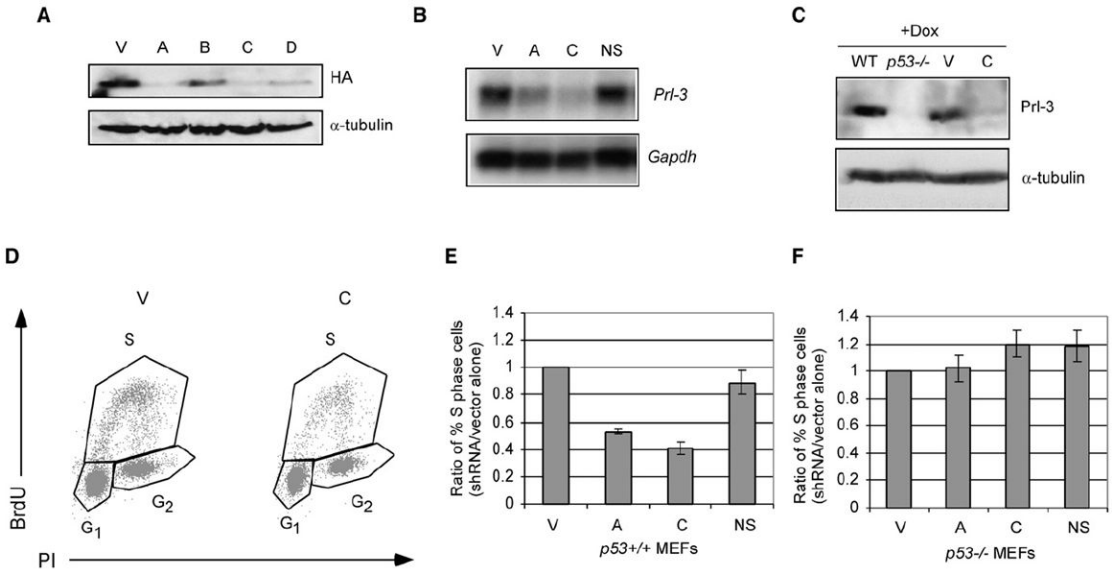

Figure 6. RNA Interference-Mediated Knockdown of Prl-3 Causes a p53-Dependent Arrest in Unstressed MEFs

(A) Western blot analysis using HA antibodies to detect Prl-3 protein levels in H1299 cells cotransfected with the HA-Prl-3 expression plasmid, and either the pSIRIPP vector alone (V) or any of the various *Prl-3* shRNA constructs (A, B, C, or D).

(B) Wild-type MEFs infected with either pSIRIPP (V) or different shRNA retroviruses (A, C, or NS), selected for 5 days with puromycin, and treated with Dox for 20 hr were analyzed for *Prl-3* mRNA levels by northern blotting.

(C) Wild-type MEFs infected with pSIRIPP (V) or shRNA C retroviruses, selected for 5 days with puromycin, and treated with Dox for 20 hr were analyzed for Prl-3 protein by western blotting using the Prl-3 antibody. Extracts from wild-type and $p53^{-/-}$ MEFs treated with Dox for 24 hr were used as positive and negative controls for Prl-3 protein, respectively.

(D) Representative FACS analysis showing the BrdU/PI cell-cycle profile of wild-type MEFs infected with either pSIRIPP (V) or *Prl-3* shRNA C retroviruses. The gates used to quantitate the numbers of cells in the G_1, S, and G_2-M phases of the cell cycle are shown.

(E and F) Cell-cycle analysis of MEFs with Prl-3 knockdown. The percentage of S phase cells in wild-type (E) and $p53^{-/-}$ (F) MEFs infected with pSIRIPP vector viruses (V) or viruses expressing shRNAs (A, C, or NS) was quantified. The graph shows the average ratios of the percentage of S phase cells in shRNA (A, C, or NS)-expressing MEFs to the percentage of S phase cells in MEFs transduced with empty vector viruses (V) from three different experiments, ± SEM.

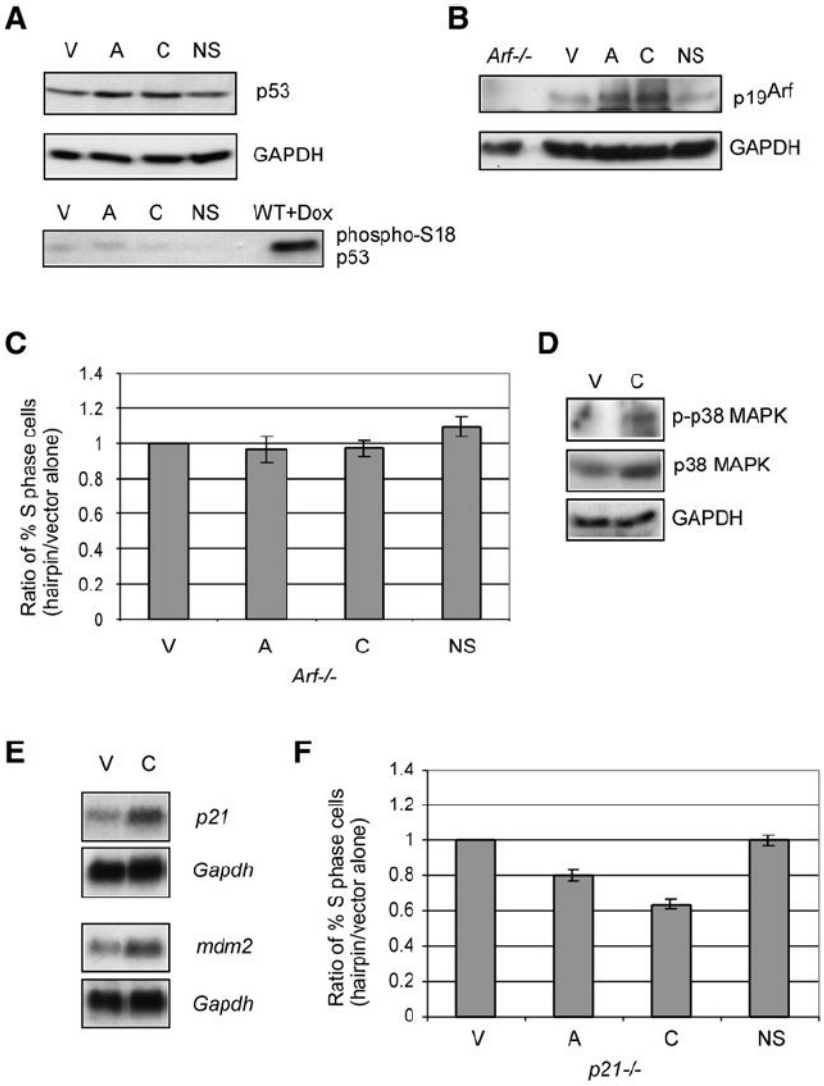

Figure 7. Prl-3 Knockdown Leads to p53 Activation in Unstressed MEFs

(A) p53 protein levels increase with Prl-3 knockdown in MEFs. Western blot analysis shows levels of total p53 or the serine 18-phosphorylated form of p53 in wild-type MEFs infected with pSIRIPP (V) or shRNA retroviruses (A, C, or NS). Extracts from wild-type MEFs treated with Dox (WT+Dox) were used as a positive control for p53 S18 phosphorylation.

(B) Prl-3 knockdown leads to $p19^{Arf}$ induction. Western blot analysis shows $p19^{Arf}$ protein levels in wild-type MEFs infected with pSIRIPP (V) or shRNA retroviruses (A, C, or NS). Extracts from $p19^{Arf-/-}$ MEFs were used to verify the identity of $p19^{Arf}$.

(C) Cell-cycle arrest upon Prl-3 knockdown is completely compromised in $p19^{Arf-/-}$ MEFs. The percentage of S phase cells in $p19Arf^{-/-}$ MEFs infected with pSIRIPP vector viruses (V) or viruses expressing the A, C, or NS shRNAs was quantified. The graph shows the average ratios of the percentage of S phase cells in A, C, or NS shRNA-expressing MEFs to the percentage of S phase cells in MEFs transduced with empty vector viruses (V) from three different experiments, ± SEM.

(D) Prl-3 ablation leads to the activation of p38 MAPK. Western blot analysis shows the levels of total p38 MAPK and phospho-p38 MAPK in wild-type MEFs infected with pSIRIPP (V) or *Prl-3* shRNA C (C) retroviruses.

(E) p53 transcriptional activity is augmented in MEFs with Prl-3 knockdown. Northern blot analysis shows *p21* and *mdm2* mRNA levels from wild-type MEFs infected with pSIRIPP (V) or *Prl-3* shRNA C (C) retroviruses.

(F) Analysis of $p21^{-/-}$ MEFs shows that p21 is required for a complete Prl-3 knockdown-mediated arrest. The graph is as described in (C).